A Sub-Domain Inverse Finite Element Characterization of Hyperelastic Membranes Including Soft Tissues

Padmanabhan Seshaiyer
Department of Mathematics and Statistics,
Texas Tech University, Lubbock, TX 79409-1042

Jay D. Humphrey*
Department of Biomedical Engineering,
Texas A&M University,
College Station, TX 77843-3120

Quantification of the mechanical behavior of hyperelastic membranes in their service configuration, particularly biological tissues, is often challenging because of the complicated geometry, material heterogeneity, and nonlinear behavior under finite strains. Parameter estimation thus requires sophisticated techniques like the inverse finite element method. These techniques can also become difficult to apply, however, if the domain and boundary conditions are complex (e.g. a non-axisymmetric aneurysm). Quantification can alternatively be achieved by applying the inverse finite element method over sub-domains rather than the entire domain. The advantage of this technique, which is consistent with standard experimental practice, is that one can assume homogeneity of the material behavior as well as of the local stress and strain fields. In this paper, we develop a sub-domain inverse finite element method for characterizing the material properties of inflated hyperelastic membranes, including soft tissues. We illustrate the performance of this method for three different classes of materials: neo-Hookean, Mooney Rivlin, and Fung-exponential. [DOI: 10.1115/1.1574333]

Keywords: Membrane Theory, Marquardt Regression, Newton-Raphson Method

Introduction

When quantifying the stress-strain behavior of a material, one typically seeks experiments that correspond to tractable boundary value problems. Prime examples in finite elasticity include uniaxial and biaxial stretching tests wherein one focuses on a gage length or central region in order to avoid complexities due to "edge effects." That the deformation is homogeneous, or nearly so, in the central region is advantageous both theoretically and experimentally—it renders the boundary value problem trivial and it ensures that the inherent averaging in the measurements (which are always over finite, rather than infinitesimal, lengths) represents well the actual values of stress and strain. In some cases, however, the investigator does not have control over the experimental conditions. For example, there may be a need to evaluate nondestructively the properties of an elastomeric structure in its service condition or to quantify the behavior of a biological soft tissue while preserving its native geometry. In such cases, where the associated boundary value problem is complex, one often employs the inverse finite element method [1–3]. Briefly, nonlinear inverse finite element methods require the solution of a forward finite element problem (e.g., solve for displacements given the loads and material properties) for many different values of the material parameters until the solution matches well the associated experimental measurements (e.g., displacements). To facilitate a judicious choice of the material parameters, one couples the finite element solution with a nonlinear regression algorithm that estimates the "best-fit" material parameters by comparing each finite element solution to the experimental data in a (nonlinear) least squares sense.

Although the inverse finite element method has become the method of choice in many areas of experimental mechanics, it is not without shortcomings. In particular, in cases wherein the material is heterogeneous, it could be nearly impossible to find simultaneously a unique set of material parameters for many different regions. Likewise, it can be difficult to measure, and thus prescribe exactly, the requisite boundary conditions over the entire physical domain. In the spirit of that which the experimentalist desires, therefore, we suggest that it can be advantageous to apply the inverse finite element method over separate sub-domains rather than the entire domain. That is, one can define a sub-domain via a small number of interconnected finite elements within a small region wherein measurements are to be made and then prescribe as boundary conditions the appropriate values (e.g., displacements) of the outer nodes that define the sub-domain; hence, the nonlinear regression can be performed by comparing finite element determined values at the inner nodes within the sub-domain with their experimental counterparts to find the "best-fit" material parameters. Not only does this sub-domain approach avoid difficulties associated with measuring all of the boundary conditions for the entire domain, it also allows one to calculate a small (or single, assuming local homogeneity) set of material parameters in each estimation. One can map overall material heterogeneity, of course, by simply repeating the analysis over multiple sub-domains, that is, regions of interest. Finally, this sub-domain approach is also consistent with the experimental reality that it is easier to measure quantities at a small number of locations on a structure at multiple equilibrium configurations rather than to measure quantities at all locations on a structure at only a few equilibrium configurations. Indeed, for nonlinear behavior, one must make measurements over the full range of strains of interest, that is, for many equilibrium configurations. Hence, again, the proposed sub-domain method is not only computationally more efficient than a full inverse method, it is consistent with standard practice in experimental finite elasticity, the focus herein.

To illustrate the sub-domain approach, we present numerical simulations for pressurized hyperelastic membranes, including biological soft tissues. In particular, we demonstrate the utility of

*Address for correspondence: J. D. Humphrey, Department of Biomedical Engineering, 233 Zachry Engineering Center, Texas A&M University, College Station, TX 77843-3120 Tel: (979) 845-5558, Fax: (979) 845-4450, e-mail: jhumphrey@tamu.edu

Contributed by the Bioengineering Division for publication in the JOURNAL OF BIOMECHANICAL ENGINEERING. Manuscript received by the Bioengineering Division April 2002; revised manuscript received February 2003. Associate Editor: A. D. McCulloch.

a single (displacement-based) sub-domain inverse finite element approach wherein the sub-domain is defined by four, non-coplanar, triangular elements that share a common central node. The displacements of the four outer nodes are treated as boundary conditions whereas the displacement of the single inner node is compared to "experimental" data via a Marquardt-Levenberg regression that determines the best-fit values of the material parameters in a nonlinear least squares sense. Numerical simulations are presented for three different material models—neo-Hookean, Mooney-Rivlin, and Fung-exponential—and two different experimental situations, the inflation of isotropic spherical and anisotropic axisymmetric membranes. As it will be shown, the sub-domain inverse finite element method can estimate well the material parameters provided the experimental noise is not excessive and that data can be collected in multiple equilibrium configurations. Both of these conditions are consistent with implementing any similar method, and thus do not introduce new demands on the experimentalist.

Background

Membrane Constitutive Theory. An ideal elastic membrane behaves like a thin plate or shell having negligible bending stiffness. Consequently, the in-plane stresses are assumed to be uniform through the thickness of a membrane and the out-of-plane stresses are assumed to be negligible. Large elastic deformations of membranes can thus be described by the governing differential equations of motion for shells by simply neglecting all terms containing bending moments or transverse shears. These differential equations are often written in terms of the in-plane physical components of the Cauchy stress resultant tensor $\mathbf{T}$. Note, therefore that a general hyperelastic constitutive relation for a membrane can be written in physical components as [4]

$$T_{ab}=ht_{ab}=\frac{2}{J_{2D}}F_{ai}F_{bj}\frac{\partial w}{\partial C_{ij}} \tag{1}$$

where $a, b, i, j=1, 2$ and repeated indices imply summation over 1 and 2 per the usual convention. Here, t_{ab} are physical components of the Cauchy stress, F_{ai}, F_{bj} are physical components of the 2-D deformation gradient $\mathbf{F}$, $J_{2D}(=F_{11}F_{22}-F_{12}F_{21})$ is the determinant of $\mathbf{F}$, C_{ij} are physical components of the right Cauchy-Green tensor $\mathbf{C}(=\mathbf{F}^T.\mathbf{F})$, h is the thickness of the deformed membrane, and w is a 2-D strain energy function. Note that w is defined per initial surface area and it depends only on the in-plane physical components of $\mathbf{C}$. Equation (1) allows the physical components of the stress resultant to be calculated without knowing the thickness in either the deformed or undeformed configuration.

Although identification of a specific form of $w(C_{ab})$ for a given material is often very challenging (see [4]), herein we assume that such a form is known. Hence, as noted above, our focus is on calculating values of the material parameters that are embodied in a prescribed form of w.

Parameter Estimation. Best-fit values of material parameters can be determined by minimizing the error between experimental and calculated quantities, which for membranes could be either displacements or in-plane stress resultants. In either case, we minimize a nonlinear sum-of-the-squares function $\mathcal{E}$ given by the usual vector inner product as,

$$\mathcal{E}=\sum_{k=1}^{m}\{(\vec{Y}_c(\vec{b})-\vec{Y}_e).(\vec{Y}_c(\vec{b})-\vec{Y}_e)\}_k \tag{2}$$

where $\vec{Y}_e$ is a vector of *experimental* (measurable) quantities, $\vec{Y}_c(\vec{b})$ contains the *calculated* (analytically or via the finite element method) quantities, $\vec{b}$ is the vector of unknown material parameters, and m is the number of equilibrium configurations. Although several efficient strategies are available to minimize the error in (2), we adopt the Marquardt-Levenberg algorithm. It can be written as [4],

$$(\mathbf{J}^T.\mathbf{J}+\gamma\mathbf{I})^{(i)}.\Delta\vec{b}=-[\mathbf{J}^T.(\vec{Y}_c(\vec{b})-\vec{Y}_e)^{(i)}] \tag{3}$$

where, $\Delta\vec{b}=\vec{b}^{(i+1)}-\vec{b}^{(i)}$, the Jacobian $\mathbf{J}=(\partial\vec{Y}_c(\vec{b})/\partial\vec{b})^{(i)}$ for the corresponding iteration counter i, and γ is the Marquardt parameter. Note that this method requires an initial guess for $\vec{b}$, and the solution strategy depends on the size of γ in comparison to the norm of $\mathbf{J}^T.\mathbf{J}$. As the Marquardt parameter becomes large, the minimization tends towards a method of steepest descent; as it becomes small, the minimization tends towards Newton's method. This method has been shown to be robust in finite strain applications [5–6] and is readily available as the default unconstrained optimization tool, *leastsqr.m*, in the MATLAB platform.

There are, of course, other issues (besides the minimization process) that one must account for while estimating parameter values. These include, respecting requirements imposed by fundamental relations of mechanics; restricting the parameter search space used by the regression algorithm; avoiding over-parameterization; performing sensitivity analyses; determining appropriate confidence intervals for the parameters; etc. A combination of all these factors is imperative for identifying a robust constitutive descriptor [6], but our focus herein is the estimation itself.

Next, we discuss some analytical approaches to obtain the *calculated* quantities of interest. Although these are limited for most soft tissues, they motivate our subdomain approach which depends on finite element methods to obtain an approximate solution for $\vec{Y}_c$.

Analytical Approaches. The general equations governing membrane mechanics are derived easily, but their solution is often not as straightforward. In experimental investigations, therefore, the focus is often on simple geometries and loading conditions that admit homogeneous (e.g., an in-plane biaxial test) or axisymmetric (e.g., inflation or indentation) deformations [7].

For example, consider a homogeneous biaxial deformation of a planar membrane. Let $x_1=\lambda_1X_1+\kappa_1X_2$, $x_2=\kappa_2X_1+\lambda_2X_2$ and $x_3=\lambda_3X_3$, where x_a and X_A are locations of material particles in the deformed and the undeformed configurations, respectively. The parameters λ_i and $\kappa_i(i=1,2)$ can be "measured" easily by tracking the motions of multiple markers that are affixed to the surface in the central region; in a sense, then, these markers define a "sub-domain" of interest. The out-of-plane stretch ratio, λ_3, is often calculated from the incompressibility constraint ($J=\det\mathbf{F}=1$). Because of the homogeneous and planar stress field, equilibrium is satisfied identically and the membrane stresses ($\mathbf{T}_c$) can be calculated directly from (1) provided the form of the strain-energy function is known. Moreover, one can experimentally measure the principal stress resultants ($\mathbf{T}_e$) in terms of uniformly applied normal forces acting over the respective deformed lengths. These results for $\mathbf{T}_c$ and $\mathbf{T}_e$ can then be input into a stress-resultant based regression algorithm to estimate the values of the material parameters via (3). An example is in [8].

A similar approach can be followed for an axisymmetric inflation of a membrane. The governing differential equations can be solved exactly for the principal stress resultants T_i in terms of the experimentally measurable uniform distension pressure P and local principal curvatures k_i (measured using edge detection), with $i=1, 2$ denoting the respective meridional and circumferential directions. This yields $\mathbf{T}_e$. The components of the two-dimensional deformation gradient tensor $\mathbf{F}$ are also measured locally, often by tracking triplets of closely placed markers that are affixed to the surface. Again, therefore, one actually interrogates the behavior in a sub-domain. That is, provided the strain-energy function w is known, the membrane stresses ($\mathbf{T}_c$) can be calculated from (1) and this admits a stress-based estimation of the material parameters as discussed in [9].

From the preceding discussion we see that for both in-plane homogeneous and axisymmetric deformations, one can obtain solutions exactly by exploiting the simplified geometry and loads. Moreover, experimentalists naturally seek to interrogate behavior in small regions, or sub-domains. In order to test many soft-tissues in their native geometry, however, the experimental boundary value problem is much more complicated and it is often too difficult to obtain an analytical solution. One has to then employ more sophisticated methods like the finite element method to supply $\vec{Y}_c$ to the regression algorithm for estimating the values of the parameters. We submit that such finite element solutions should also be restricted to a sub-domain.

The Inverse Finite Element Method

The inverse finite element method was introduced early on [1] as an application of finite elements to characterize the mechanical properties of nonlinearly elastic solids. Since then, this method has proved to be useful in providing reasonable estimates of the best-fit values of material parameters in many cases.

General Approach. For a given undeformed configuration and boundary conditions, as well as an initial guess for the values of the material parameters, a displacement (or stress) based finite element model calculates (as a forward problem) a candidate solution and hence the requisite $\vec{Y}_c$. If, for the same undeformed configuration and boundary conditions, one can measure the displacements (or stresses) at corresponding nodal locations ($\vec{Y}_e$), then the values of $\vec{Y}_c$ and $\vec{Y}_e$ are compared via a least-squares regression method to assess the goodness of the finite element solution. If the error in the regression is within the prescribed tolerance, then the guessed parameter values are accepted as the *best-fit* values; if not, this procedure continues iteratively until good estimates are found for the material parameters. Hence the inverse finite element method, in nonlinear problems, simply requires multiple forward solutions based on updated "guesses" for the parameters from the regression algorithm. Let us now consider the direct method employed herein.

Finite Element Framework. There is an enormous literature available on finite element methods that are applicable to soft tissue mechanics [e.g. [10–14]]. Among others, these papers demonstrate the ability of finite element methods to solve various membrane inflation problems: planar, axisymmetric, and non-axisymmetric. Herein, we follow the developments in [13,14], which solve membrane inflation problems using the *principle of virtual work*. This formulation requires that the net virtual work by internal and external forces in moving through virtual displacements is zero. Mathematically, we have

$$\int_{\Omega_0} \delta w dA = \int_{\Omega} P\vec{n}.\delta\vec{x} da \tag{4}$$

where Ω_0 and Ω are the undeformed and current domains respectively, w is the strain-energy function defined per unit initial surface area A, P is the distending pressure that acts on the current configuration in the direction $\vec{n}$, and $\delta\vec{x}$ is the virtual change in the nodal positions. Equation (4) can be rewritten with respect to the undeformed configuration (i.e. a total Lagrangian formulation) and discretized using standard isoparametric shape/interpolation functions with the associated quadrature rules. The relationships hence derived result in a system of nonlinear algebraic equations that can be solved via an iterative Newton-Raphson method. Note that the nonlinearity arises due to the finite strains (geometric) as well as the constitutive relations (material). See the aforementioned papers for details.

Sub-Domain Characterization

Although standard inverse finite element methods can be very useful in characterizing soft tissues, they become very challenging when the domain is highly complex (e.g. a nonaxisymmetric aneurysm). In such cases it is difficult to estimate the material properties over the entire domain (Ω) because the material is typically heterogeneous, and imposing the boundary conditions requires measuring each, which is often a daunting task. Motivated by the standard approach in experimental mechanics, a natural alternate approach would be to solve such problems over a sub-domain ($\Omega_s \subset \Omega$), rather than over the entire domain, of the tissue. This simplification allows us to assume, in many cases, that both the material and the local stress and strain fields are homogeneous within the solution domain. This not only helps us in estimating the values of the material parameters, it also assists us in exploring possible regional variations in the material properties over the whole domain by simply considering multiple sub-domains individually. Figure 1 shows one such sub-domain Ω_s (embedded in the whole domain Ω), consisting of five non-coplanar nodes that demarcate four non-coplanar triangular elements. Since the nodes of the sub-domain Ω_s are chosen sufficiently close, the curved boundaries that connect the respective nodes can be well approximated by straight lines. It is emphasized, however, that the five nodes demarcating Ω_s must be non-coplanar to capture the curvature of an inflated membrane; for planar problems the nodes can be coplanar. Moreover, five nodes appear to be a minimally advisable set, for three nodes are required in each of the two in-plane directions to approximate the corresponding curvatures. The discretized system resulting from the principle of virtual work (i.e., the forward problem) is solved via a Newton-Raphson iterative procedure. Hence, one can obtain *calculated* ($\vec{Y}_c$) solution sets for a variety of equilibrium configurations.

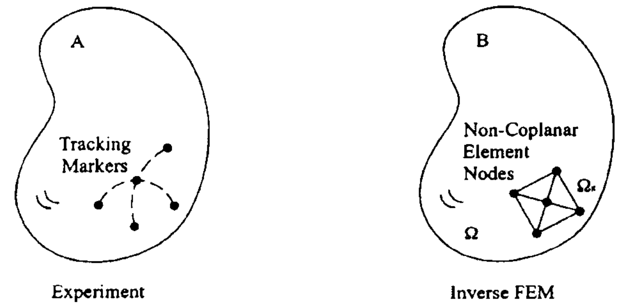

Fig. 1 Schema of a general membrane inflation. Panel A shows five markers that can be tracked experimentally using a video system whereas Panel B shows the associated four-element computational "sub-domain" $\Omega_s \subset \Omega$. The sub-domain can be made as small as allowed experimentally, and can be repeated at multiple locations on the specimen to explore possible material heterogeneities.

Just as in the case of axisymmetric inflations, one can perform non-axisymmetric membrane inflation experiments by placing markers on the surface of the specimen and tracking their positions at various pressure levels. Details of a video-based system for performing such finite strain inflation tests on biomembranes can be found in [15]. The positional data thus obtained yields the experimentally *measured* displacements ($\vec{x}_e$).

Again, therefore, calculated values ($\vec{Y}_c(\vec{b}) \equiv \vec{x}_c$) can then be compared with the experimental data ($\vec{Y}_e \equiv \vec{x}_e$) in the Marquardt-Levenberg regression algorithm to estimate values of each material parameter. Because the goal of this paper is to evaluate the potential of such estimations, we must know the true solution. Hence, we generate "experimental data" by adding random noise to a forward finite element solution as, $\vec{x}_e = \vec{x}_c \pm$ noise. The robustness of the inverse method can then be checked easily, as the estimated parameter values must be close to the parameter values that were used to calculate the forward solution $\vec{x}_c$. Of course, the finite element solution must exclude rigid body motion. This is accomplished by prescribing displacement boundary conditions. Note, therefore, that the experimentally measured marker locations ($\vec{x}_e$), at each pressure configuration, serve two functions: in the case of five markers, the outer four serve as displacement boundary conditions in the inverse finite element solution whereas the inner one serves as an experimental measurement to which the inverse finite element solution can be compared in a nonlinear least squares sense. Because each marker is located by three coordinate values, each supplies multiple pieces of information for comparing the theoretically computed and experimentally measured location. Moreover, marker positions at multiple equilibrium configurations (i.e. pressures) provides the over-determined equations needed in least squares estimations.

In order for the sub-domain problem, as presented, to be well-posed, one must prescribe carefully the boundary conditions. In other words, specifying more than the required boundary conditions on some part of the boundary, prescribing no boundary conditions, or prescribing fewer than those required might render the sub-domain problem ill-posed. Of course experimentalists are interested in the minimum number of nodes (i.e., experimental measurements) at which boundary conditions need to be specified to keep the problem well-posed.

Consider a sub-domain Ω_s consisting of n nodes. This sub-domain is partitioned into a set of non-overlapping, non-coplanar triangles Z_i (as in Fig. 1),

$$\Omega_s = Z_1 \cup Z_2 \ldots \cup Z_p$$

such that no vertex of one triangle lies on the edge of another triangle. Let us assume, too, that the elemental stiffness matrices can be computed easily as in [13,14]. These local elemental matrices are then assembled to build the global system consisting of $3n$ equations and $3n$ unknowns (with 3 displacements per node). Let N be the number of *free* nodes on which the minimization will be performed in all three directions. Hence, we treat $n-N(=L)$ nodes to be *fixed*, that is, where the displacement boundary conditions are prescribed. The global system can thus be written as,

$$\begin{bmatrix} \mathbf{K}_1 & \mathbf{K}_2 \\ \mathbf{K}_3 & \mathbf{K}_4 \end{bmatrix} \begin{bmatrix} q^F \\ q^{NF} \end{bmatrix} = \begin{bmatrix} Q_1 \\ Q_2 \end{bmatrix} \tag{5}$$

where the block matrices $\mathbf{K}_1$ of size $3N \times 3N$, $\mathbf{K}_2$ of size $3N \times 3L$, $\mathbf{K}_3$ of size $3L \times 3N$ and $\mathbf{K}_4$ of size $3L \times 3L$ are components of the tangent stiffness matrix; $\mathbf{q}^F$ and $\mathbf{q}^{NF}$ are the positions corresponding to the nodes that are *fixed* and *not fixed* respectively; $\mathbf{Q}_1$ and $\mathbf{Q}_2$ are the components of the load vector. By prescribing the boundary conditions, the above system can be (partitioned) reduced to,

$$\mathbf{K}\; q^{NF} = f \tag{6}$$

where,

$$\mathbf{K} = \mathbf{K}_4 - \mathbf{K}_3 \mathbf{K}_1^{-1} \mathbf{K}_2 \tag{7}$$

and

$$f = \mathbf{Q}_2 - \mathbf{K}_3 \mathbf{K}_1^{-1} \mathbf{Q}_1 . \tag{8}$$

Hence a *sufficient condition* for choosing the number of *free* nodes would be to guarantee that the matrices $\mathbf{K}_1$ and $\mathbf{K}$ are non-singular. It can be shown that this condition is equivalent to selecting well the strain-energy function w (e.g. convex). Since the form of w dictates the number of the material parameters, the singularity condition also restricts the parameter search space.

Illustrative Results

Let us now consider results for three specific classes of materials: neo-Hookean, Mooney-Rivlin and Fung-exponential. These material models are not necessarily the best descriptors of membrane behavior under finite strain, they are simply commonly used.

Forms of Strain-Energy Functions. The 3-D *Mooney-Rivlin* model is given by,

$$W = c_1[(I_1 - 3) + \Gamma(I_2 - 3)] \tag{9}$$

where c_1 (having units of stress) and Γ (dimensionless) are material parameters and I_1, I_2 are principal invariants of the right Cauchy-Green tensor $\mathbf{C}$. Note that $w = WH$ where H is the thickness of the undeformed membrane; it is also convenient then to let $c \equiv c_1 H$. When $\Gamma = 0$, (9) becomes a *neo-Hookean* model.

For membranous soft tissues, however, the *Fung-exponential* model is often used. It is,

$$w = c(e^Q - 1) \tag{10}$$

where $Q = c_1 E_{11}^2 + c_2 E_{22}^2 + 2c_3 E_{11} E_{22}$ and E_{11}, E_{22} are principal components of the 2D Green strain tensor $\mathbf{E} = 0.5(\mathbf{C} - \mathbf{I})$. Here, c is a material parameter having units of force/length and c_1, c_2 and c_3 are dimensionless. The Fung-exponential model can also be written for the case of isotropy ($c_1 = c_2$) in terms of the invariants of the 2-D Green strain, J_1 and J_2, as

$$w = c(e^{\alpha J_1^2 + 2\beta J_2} - 1) \tag{11}$$

where c, α and β are the material parameters.

Results for Inflated Spheres. Let a sub-domain Ω_s on the surface of a thin-walled sphere (domain Ω) be demarcated by five non-coplanar nodes (Fig. 2*A*), each defined by undeformed coordinates (R, Θ, Φ). This defines four linear but non-coplanar triangular elements, each sharing one common node. Let the sphere be

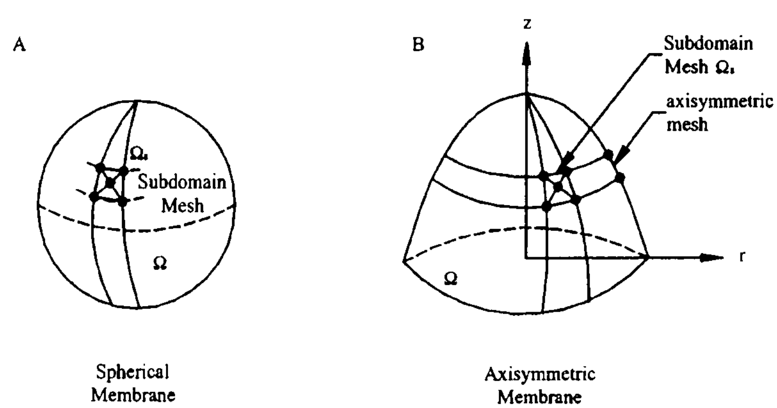

Fig. 2 Schema showing a possible four element sub-domain on an inflated sphere (panel A) and an axisymmetrically inflated membrane (panel B). The latter also shows a three noded element used in the forward problem in an axisymmetric finite element solution.

PROOF COPY 011303JBY

isotropic in its response and inflated by an uniform distension pressure P; each node thus displaces to its new position (r, θ, ϕ).

Due to axisymmetry, the current coordinates and the undeformed coordinates will be related as, $r = r(R)$, $\theta = \Theta$, $\phi = \Phi$. For this perfectly spherical geometry, we also know that the principal stretch ratios and the curvatures respectively satisfy, $\lambda_1 = \lambda_2 = r/R$ and $k_1 = k_2 = 1/r$. The out-of-plane stretch ratio is calculated from material incompressibility $\lambda_3 = h/H = 1/\lambda^2$, with $\lambda = r/R$. Once the specific form of the strain-energy function w is known, the principal stress resultants T_1 and T_2 can be derived as a function of λ from (1). Note that the distension pressure P can also be calculated as, $P(\lambda) = 2T(\lambda)/r$, where $T(\lambda) = T_1(\lambda) = T_2(\lambda)$.

Figure 3 (top; middle) illustrates the response of a spherical neo-Hookean membrane (R=2.5 mm) under inflation as a function of the uniform stretch ratio $\lambda \in [1.1, 1.2]$. The exact solution for the stress resultant from (1) and (9), with $\Gamma = 0$, is

$$T(\lambda) = 2Hc_1\left(1 - \frac{1}{\lambda^6}\right). \tag{12}$$

We non-dimensionalize the pressure as $P^* = PR/c$ and the stress resultant as $T^* = T/c$. Experimental data were simulated by adding Gaussian noise, with a mean of 0.0 and standard deviation of 0.01 mm (with respect to the size of the sphere), to the deformed positions. The sub-domain method was then used to estimate the single material parameter. We show $c^* = c/c_t$, where c_t is the true value (i.e., value used in the forward problem to generate the data). We will denote the true value of the material parameter by a solid line in all the graphs from hereon. Figure 3 (bottom) shows that the sub-domain inverse finite element estimated parameter approached the true value with increasing pressurization (i.e., stretch).

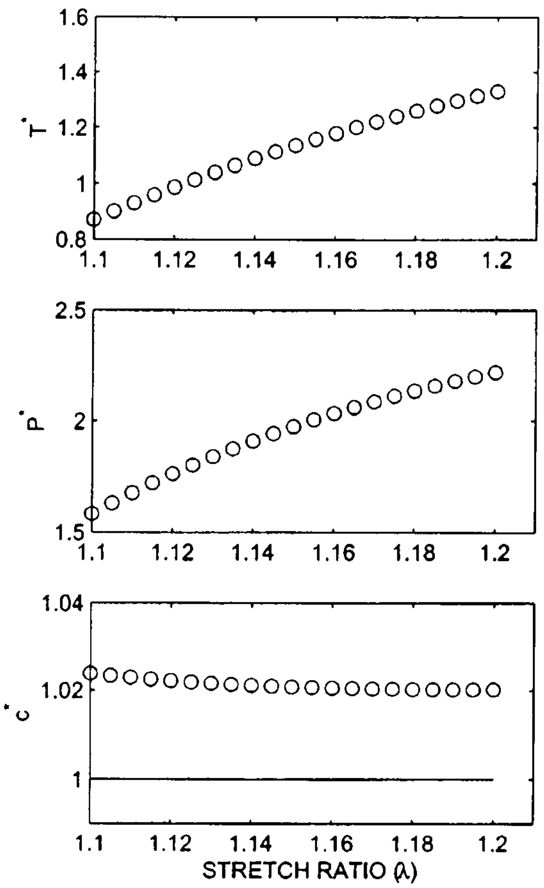

Fig. 3 Results for the inflation of a neo-Hookean spherical membrane as a function of the in-plane stretch λ. The top and middle panels show the material response for moderate stretches, less than that associated with a limit point instability ($\lambda = 7^{1/6}$). The bottom panel shows the estimated value of the neo-Hookean parameter for increasing values of λ, which includes increasing numbers of equilibrium configurations.

Given that the increasing stretch in Fig. 3 also corresponds to increasing the number of equilibrium configurations—which is easier for the experimentalist to achieve than increasing the data collected at each configuration—the utility of this was evaluated for each of the three models. The normalized material parameters for each model are plotted in Fig. 4, 5 and 6, respectively, for 20 equilibrium configurations up to a maximum pressure of 160 mmHg. The true values of the dimensionless parameters were $\Gamma = 0.89$ for the Mooney-Rivlin model and $\alpha = 0.2$, $\beta = 1.0$ for the Fung-exponential model. These figures show that the estimated material parameters (for the respective models) approached the true values as the number of equilibrium configurations increased, thereby reducing the error associated with the parameter estimation.

Perhaps the greatest impediment to robust parameter estimation is the presence of experimental noise [1]. Hence, we tested the performance of our method for all three models using different *levels of experimental noise* (standard deviation from 3×10^{-2} mm to 1×10^{-4} mm, which was added to the forward solution to generate data for the inverse problem). The results are

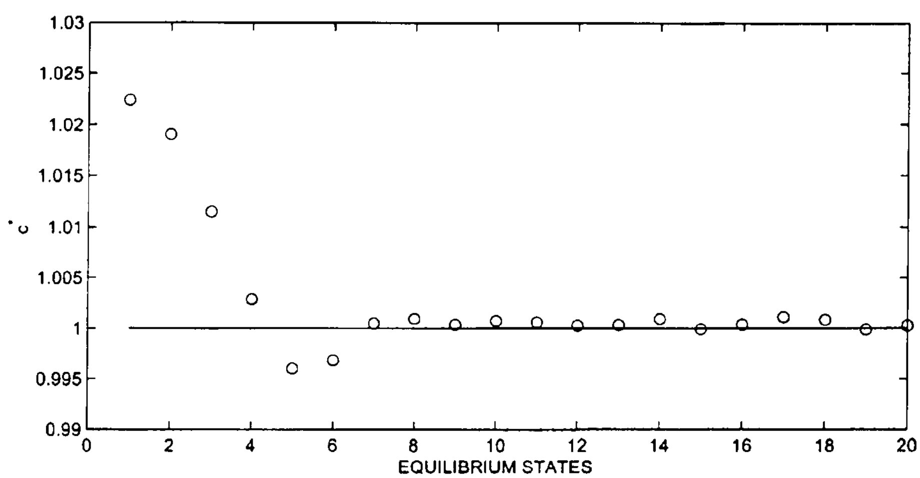

Fig. 4 Estimated parameter values versus number of equilibrium configurations for a neo-Hookean sphere inflated to a stretch of 1.33; noise is 0.01.

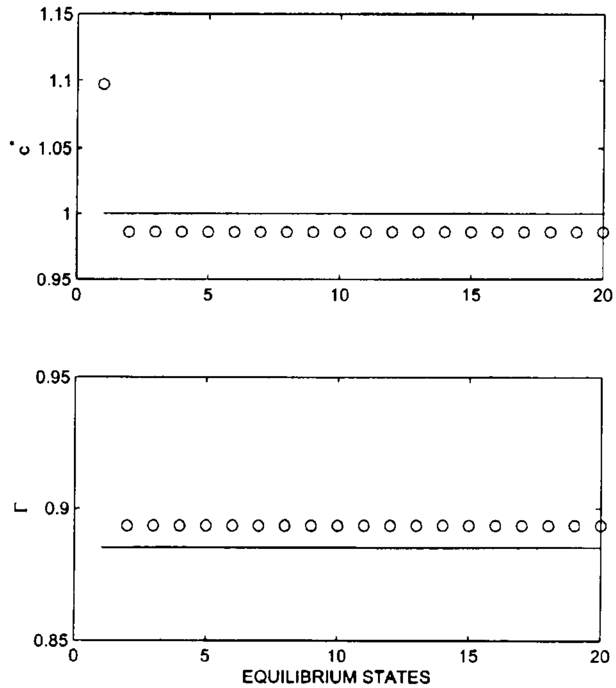

Fig. 5 Similar to Figure 4 except for a Mooney-Rivlin sphere inflated to a stretch of 1.33 ($\Gamma=0.89$); noise is 0.01.

shown in Fig. 7, 8 and 9, respectively, for each model. Although all the results seem to behave as expected (i.e. the relative error in the estimated material parameters increased markedly with an increase in experimental noise), note that the error in parameter estimation is the least for the neo-Hookean model and greatest for the Fung-exponential model. One reason for this is the number of material parameters in each model: 1 for neo-Hookean (c), 2 for Mooney-Rivlin (c,Γ) and 3 for Fung-exponential (c,α,β). As expected, testing the robustness of a multiparameter constitutive relation is a more severe test for the parameter estimation and experimental errors will play a more influential role in such cases. The behavior of the error in the parameter estimation for the Fung-exponential model is also due to the exponential term, which is very sensitive to experimental noise, and co-linearity between c and the exponential parameters.

Of course, it is desirable to prescribe an acceptable bound for the size of the sub-domain Ω_s in comparison to the size of the entire domain Ω. For this, we inscribed the sub-domain Ω_s inside a circle of radius ρ, which was defined by the maximum distance between the center and the other nodes. We performed parameter estimations for each model by varying the ratio ρ/R. It was observed that the tangent-stiffness matrix in (6) becomes singular if the ratio becomes greater than 0.1, thus confirming that experimental regions of interest must be "small" to ensure goodness of the approximation afforded by linear triangular elements. It must be noted, however, that this bound would depend on the specific form of the strain-energy function.

General Axisymmetric Inflations. So far, we have considered simulated experimental data for the case of the uniform inflation of an isotropic spherical membrane. This simple boundary value problem can be considered as a convenient *patch test* for our method. A more stringent test, however, is provided by the inflation of an axisymmetric membrane having regional variations in material properties. Such a problem corresponds to that of a sub-class of idealized saccular aneurysms—with a material symmetry that varies linearly from isotropic at the pole to maximally orthotropic at the base—as studied in [16]. Here, we will simply add random noise to the computed nodal displacements and use

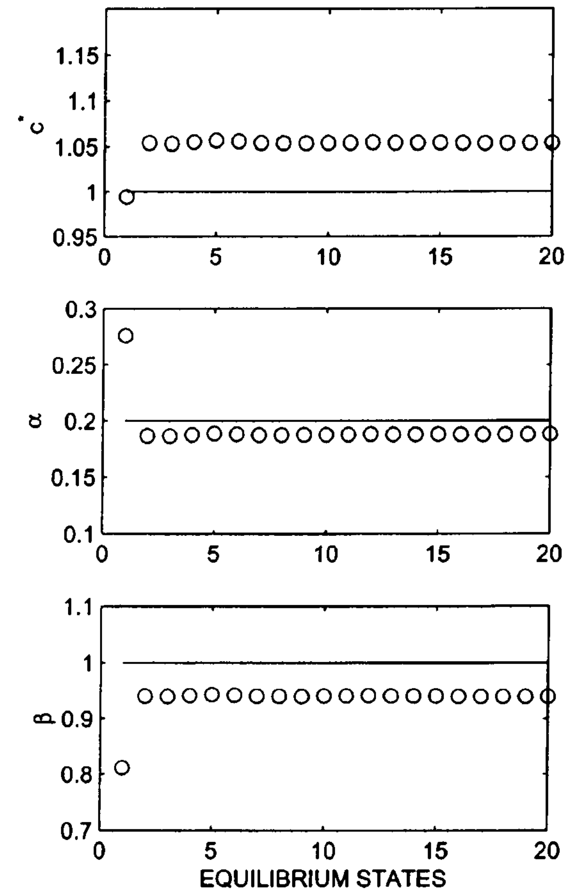

Fig. 6 Similar to Figure 4 except for a Fung-exponential sphere inflated to a stretch of 1.1 ($\alpha=0.2, \beta=1.0$); noise is 0.01.

these "data" as input to our sub-domain inverse finite element code. Briefly, in [16], both the undeformed and the deformed configurations were described by generator curves that were rotated about a common axis. Cylindrical coordinates were used to map a material particle at (R,Z) in the undeformed configuration to (r,z) in the deformed configuration ($\theta=\Theta$ for axisymmetry). The undeformed (R,Z) and the deformed (r,z) positions were approximated via isoparametric interpolation [17]. The interpolation functions were taken to be quadratic in ζ with the center node at $\zeta=0$ (Figure 2B).

To generate experimental data from a forward problem, we chose a single element along the arc length and rotated the nodes in θ to obtain a five noded sub-domain (similar to the one on the surface of the sphere) in both the undeformed and the deformed configurations (Fig. 2B). Noise was then added randomly to the displacements of each of the five nodes defining the sub-domain and the resulting locations served as experimental data ($\vec{x}_e$). We also computed the finite element solution (from our code) for the same set of undeformed coordinates and the pressure configuration with displacement boundary conditions specified at the outer four nodes of the five noded sub-domain, again keeping the common center node as a *free* node. The initial guess of the values of material parameters were chosen in such a way that convergence is guaranteed in the solution. The solution hence computed served as the *calculated* ($\vec{x}_c$) data that were compared with the experimental data ($\vec{x}_e$) in a least-square sense.

For purposes of illustration, let the total number of elements used in [16] be 24 and the material model be Fung-exponential. The simulation was performed for 20 increasing equilibrium configurations up to a maximum pressure of 160 mmHg. Moreover,

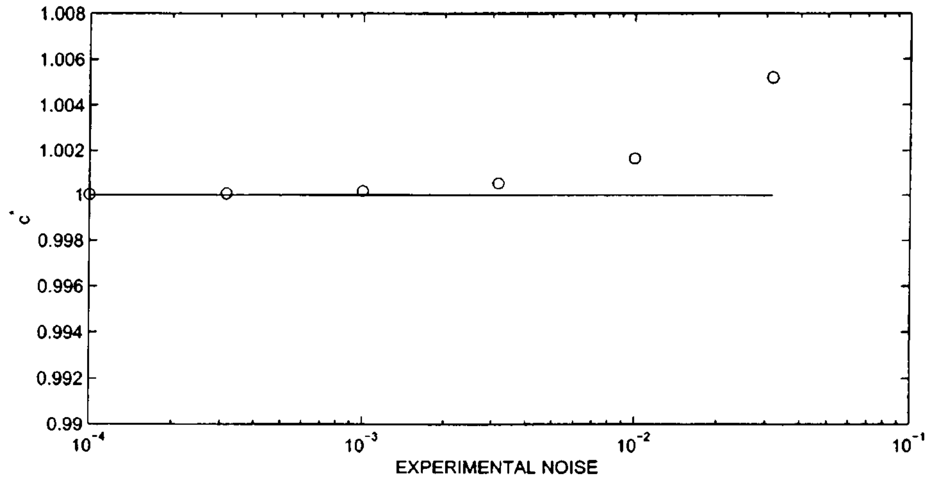

Fig. 7 Estimated parameter values as a function of increasing experimental noise for a neo-Hookean sphere inflated to a stretch of 1.33 via 10 equilibrium configurations.

consider a membrane exhibiting orthotropy. The Fung-exponential strain-energy function can be expressed, using (10), with

$$Q = c_2 J_1^2 + 2(c_3 - c_2)J_1 J_4 + (c_1 + c_2 - 2c_3)J_4^2 \tag{13}$$

where J_1 and J_4 are invariants of the Green strain. In order to allow regional variations in anisotropy, the ratio c_2/c_1 was allowed to vary from element to element as,

$$\frac{c_2}{c_1} = 1 - (1 - M)\frac{(le - 1)^p}{(ne - 1)^p} \tag{14}$$

where le is the local element, ne is the total number of elements, p is the order and $M = c_2/c_1|_{\max}$, the ratio at the base of the inflated membrane.

From [3], the true values of the material parameters were $c = 0.8769$ N/m, $c_1 = 4.50$ and $c_3 = 1.18$. We first estimated the values of the material parameters using our inverse finite element method over the 4 element sub-domain corresponding to element 10 in the forward problem. From (14), the value of c_2 is calcu-

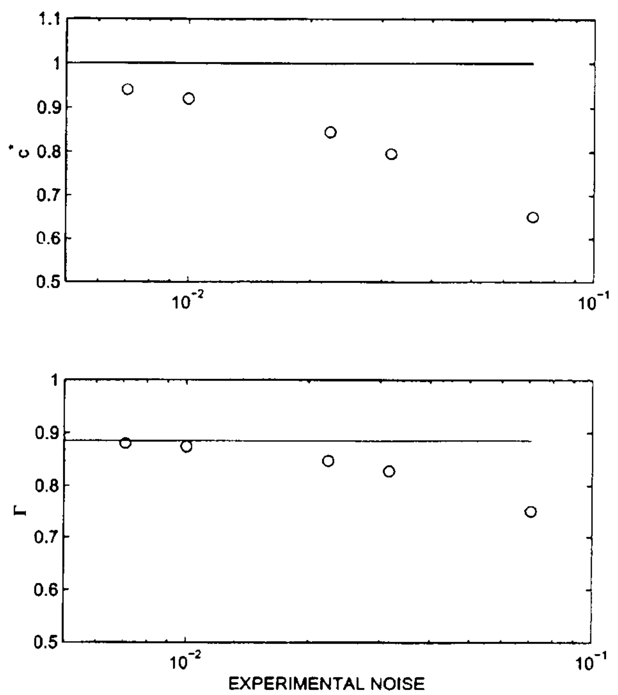

Fig. 8 Similar to Figure 7 except for a Mooney-Rivlin sphere inflated to a stretch of 1.33 via 10 equilibrium configurations.

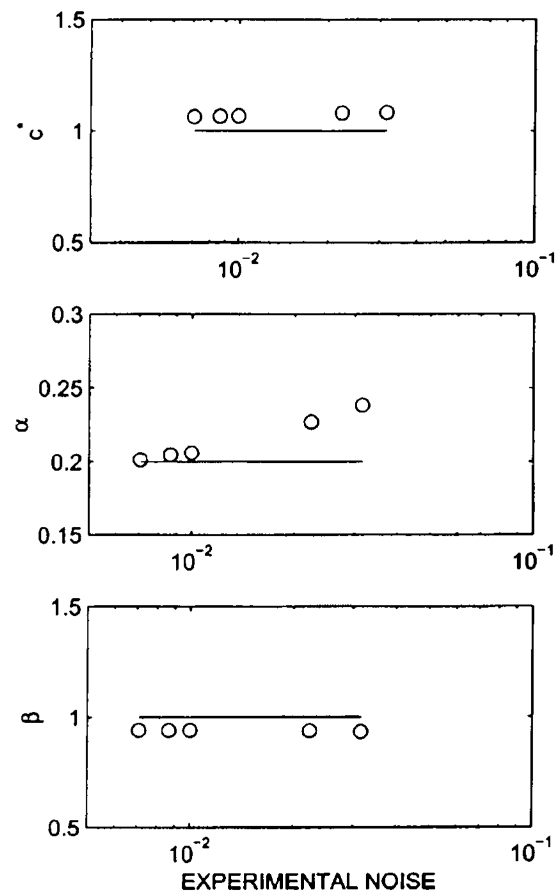

Fig. 9 Similar to Figure 7 except for a Fung-exponential sphere inflated to a stretch of 1.05 via 10 equilibrium configurations.

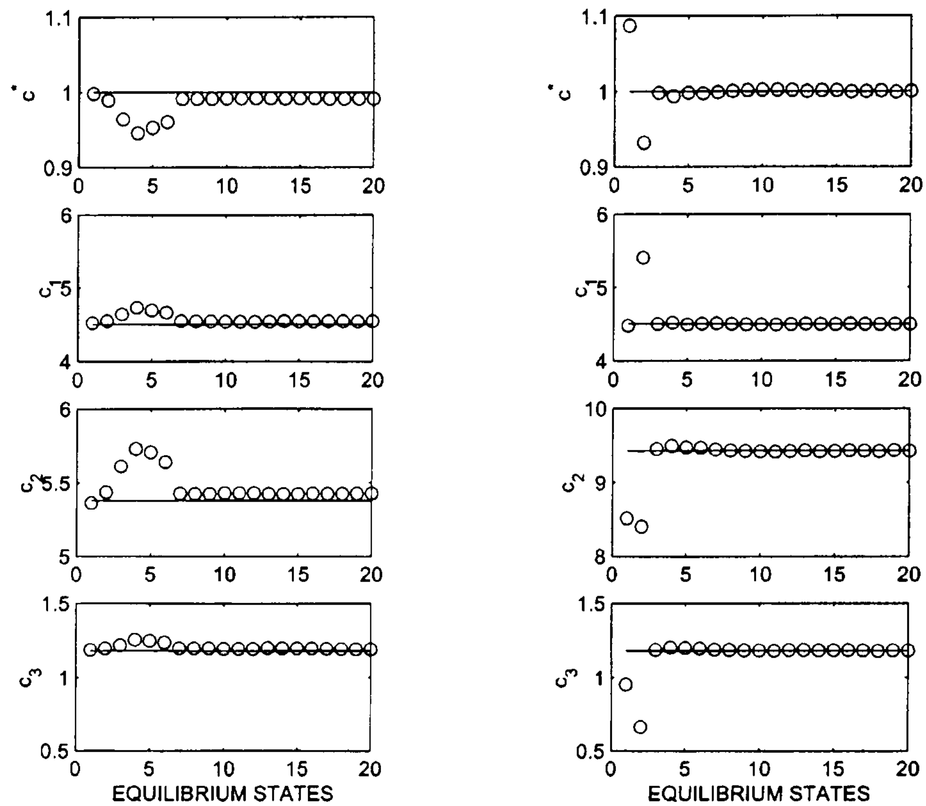

Fig. 10 Estimated parameter values for an orthotropic Fung-exponential material over element 10 (left panels) and over element 17 (right panels). See text for details.

lated over the local element 10 (with $p=3$ and $M=4.25$) to be 5.37. The left panels in Fig. 10 (left panels) shows how well each of the material parameters c, c_1, c_2 and c_3 are estimated by our scheme as the number of equilibrium configurations increases.

In order to demonstrate the performance of our method with regional variations in material parameters over the entire domain, we repeated our simulations on a 4 element sub-domain formed by element 17 in the forward problem. The true values of c, c_1 and c_3 are the same as before while the value of c_2 can be calculated from (14) to be 9.42. Figure 10 (right panels) once again illustrates how closely the values of the material parameters are estimated to the true values with increasing number of equilibrium configurations. For completeness, we also considered a material exhibiting isotropy ($c_1=c_2$) which can be implemented by choosing $M=1$ in (14). We used $c=0.8769$ N/m, $c_1=c_2=11.82$ and $c_3=1.18$ as the true values to simulate this isotropic behavior. Once again, there was an excellent recovery of the material parameters (not shown).

Conclusion

The numerical results presented in this paper suggest that one can employ inverse finite element methods over sub-domains rather than the entire domain to determine membrane properties when the associated boundary value problem is complex. With this technique one can now quantify the mechanical behavior of complex soft-tissues like intracranial saccular aneurysms and also design the requisite experiments. This technique allows characterization of the regional variations in these properties.

Acknowledgements

This work was supported by a grant from the National Institutes of Health (HL 54957).

References

[1] Kavanaugh, K. T., and Clough, R. W., 1971, "Finite Element Applications in the Characterization of Elastic Solids," Int. J. Solids Struct., **7**, pp. 11–23.
[2] Iding, R. H., Pister, K. S., and Taylor, R. L., 1974, "Identification of Nonlinear Elastic Solids by a Finite Element Method," Comput. Methods Appl. Mech. Eng., **4**, pp. 121–142.
[3] Kyriacou, S. K., Shah, A. D., and Humphrey, J. D., 1997, "Inverse Finite Element Characterization of Nonlinear Hyperelastic Membranes," J. Appl. Mech., **64**, pp. 257–262.
[4] Humphrey, J. D., 1998, "Computer Methods in Membrane Biomechanics," Computer Methods in Biomechanics and Biomedical Engineering, **1**, pp. 171–210.
[5] Twizell, E. H. and Ogden, R. W., 1983, "Nonlinear Optimization of the Material Constants in Ogden's Stress-deformation Function for Incompressible Isotropic Elastic Materials," J. Austral. Math. Soc., **24**, pp. 424–434.
[6] Humphrey, J. D., Strumpf, R. K., and Yin, F. C. P., 1990, "Determination of a Constitutive Relation for Passive Myocardium: II. Parameter Estimation," ASME J. Biomech. Eng., **112**, pp. 340–346.
[7] Humphrey, J. D., 2002, Cardiovascular Solid Mechanics: Cells, Tissues, and Organs, Springer-Verlag, NY.
[8] Humphrey, J. D., Strumpf, R. K., and Yin, F. C. P., 1992, "A Constitutive Theory for Biomembranes: Application to Epicardium," ASME J. Biomech. Eng., **114**, pp. 461–466.
[9] Hsu, F. P. K., Schwab, C., Rigamonti, D., and Humphrey, J. D., 1994, "Identification of Response Functions for Nonlinear Membranes via Axisymmetric Inflation Tests: Implications for Biomechanics," Int. J. Solids Struct., **31**, pp. 3375–3386.
[10] Oden, J. T., and Sato, T., 1967, "Finite Strains and Displacements of Elastic Membranes by the Finite Element Method," Int. J. Solids Struct., **3**, pp. 471–488.
[11] Oden, J. T., 1972, Finite Elements of Nonlinear Continua., McGraw-Hill, NY.
[12] Wriggers, P., and Taylor, R. L., 1990, "A Fully Nonlinear Axisymmetrical Membrane Element for Rubber-like Materials," Eng. Comput., **7**, pp. 303–310.
[13] Gruttmann, F., and Taylor, R. L., 1992, "Theory and Finite Element Formulation of Rubberlike Membrane Shells Using Principal Stretches," Int. J. Numer. Methods Eng., **35**, pp. 1111–1126.
[14] Kyriacou, S. K., Schwab, C., and Humphrey, J. D., 1996, "Finite Element Analysis of Nonlinear Orthotropic Hyperelastic Membranes," Computational Mechanics, **18**, pp. 269–278.

[15] Hsu, F. P. K., Downs, J., Liu, A. M. C., Rigamonti, D., and Humphrey, J. D., 1995, "A Triplane Video-based Experimental System for Studying Axisymmetrically Inflated Biomembranes," IEEE Trans. Biomed. Eng., **42**, pp. 442–449.

[16] Shah, A. D., Harris, J. L., Kyriacou, S. K., and Humphrey, J. D., 1997, "Further Roles of Geometry and Properties in the Mechanics of Saccular Aneurysms," Computer Methods in Biomechanics and Biomedical Engineering, **1**, pp. 109–121.

[17] Fried, I., 1982, "Finite Element Computation of Large Rubber Membrane Deformations," Int. J. Numer. Methods Eng., **18**, pp. 653–660.